ISSN 0001-4338, Izvestiya, Atmospheric and Oceanic Physics, 2024, Vol. 60, No. 9, pp. 1060–1074. © Pleiades Publishing, Ltd., 2024.
Russian Text © The Author(s), 2024, published in Issledovanie Zemli iz Kosmosa, 2024, No. 3, pp. 59–77.

USING SPACE INFORMATION ABOUT THE EARTH
EXPLORATION OF THE AQUATIC ENVIRONMENT FROM SPACE

Features of the Structure and Dynamics of Waters in the Northern Half of the Sea of Japan in the Autumn–Winter Period According to Satellite and Ship Observations

A. F. Sergeev[a, *], V. B. Lobanov[a], V. A. Goryachev[a], N. V. Shlyk[a], E. N. Maryina[a], N. B. Lukyanova[a], I. I. Gorin[a], V. Tsoy[a], S. A. Zverev[a], A. Yu. Yurtsev[b], I. A. Prushkovskaya[a], and S. Yu. Ladychenko[a]

[a] *Il'ichev Pacific Oceanological Institute, Far Eastern Branch, Russian Academy of Sciences, Vladivostok, 690041 Russia*
[b] *National Research Fleet Manager, Vladivostok, Primorskii krai, 690091 Russia*
**e-mail: sergeev@poi.dvo.ru*
Received October 31, 2023

Abstract—This article presents the results of studies of the structure and dynamics of waters in the large-scale cyclonic gyre (LSCG) zone in the northern half of the Sea of Japan, where two areas of low temperatures separated by the influx of warm Tsushima waters from Japan are most clearly visible on satellite IR images every autumn–winter period. The location of these thermal structures coincides with the location of the small western and northern cyclonic gyres, which are inextricably linked with deep upwelling. In the autumn–winter periods of 2019–2021, it was established that deep upwelling in the northwestern part of the Sea of Japan extends from the bottom to the surface layer, focusing along the axial line passing through the Pervenets Rise and the Bersenev and Vasilkovsky ridges in the region of 42° N between 132° E and 135.5° E. The cyclonic gyre (WCG) located in the western part of the LSCG in the area of deep upwelling under consideration is a large topographic eddy. In the northern part of the LSCG, the deep upwelling is confined to the continental clone, where the northern cyclonic gyre (NCG) is also located. It is assumed that in the autumn–winter period, the interaction of anticyclones that form vortex belts with cyclonic gyres leads to an increase in deep circulation. The peculiarity of the variability of the velocity of deep currents—an increase from October to March—is probably due to the developmental nature of vertical and transverse horizontal circulation in the system of cyclonic gyre–vortex belt system as a result of the intensification of deep upwelling with the strengthening winds from northern directions in winter.

Keywords: infrared satellite images, anomalous thermal areas, upwelling, cyclonic gyres, topographic eddy, anticyclonic eddies, vertical and transverse horizontal circulation

DOI: 10.1134/S0001433824701020

INTRODUCTION

The use of infrared satellite images in the study of the northern half of the Sea of Japan has made it possible to significantly develop our understanding of the structure and dynamics of fronts, currents, synoptic eddies, and coastal upwelling (Zhabin et al., 1993; Yurasov, 1995; Lobanov et al., 2007; Nikitin et al., 2009; Nikitin and Yurasov, 2017). This became possible due to the peculiarity of the satellite method: it allows one to simultaneously and repeatedly during the day obtain images with a detailed distribution of sea surface temperature (SST) for the entire sea area and observe the emergence and evolution of multiscale thermal structures. Two such structures, which are most clearly visible on satellite images annually in the autumn–winter period, are observed in the large-scale cyclonic gyre (LSCG). Satellite IR images obtained from the website http://www.satellite.dvo.ru and presented in Fig. 2 show that, in the autumn–winter months of 2019 and 2021 (data from the expeditions of these years are used in this study), the two large-scale areas of low temperature were formed in the northern half of the sea, separated by the influx of warm Tsushima waters from Hokkaido Island. The southwestern area is approximately located between 130°–135° E in longitude and from the coast to the subarctic front at 40° N in latitude; the northeastern area is between 135°–139° E and 43°–46° N. With the change from the summer monsoon to the winter one and the emergence of autumn wind coastal upwelling (Goncharenko et al., 1993; Zhabin et al., 1993; Yurasov, 1995), conditions are created for a rapid decrease in SST over a vast area of water due to mixing in the upper layer of the sea with an increase in headwinds, a seasonal decrease in air temperature, and the removal of cold transformed upwelling waters from the coast. One of the factors leading to the formation of two thermal regions, in addition to those listed above, may be a phenomenon that has not been sufficiently studied at the moment: the rise of deep waters (deep upwelling of the open sea), observed throughout the year in the northern half of the Sea of Japan in the area of LSCG, which is identified in sections by the dome-shaped configuration of isolines of hydrological and hydrochemical parameters (Leonov, 1960; Mokievskaya, 1961; Panfilova, 1961; Pokudov et al., 1976; Yurasov and Yarichin, 1991; Talley et al., 2004). In addition to cyclonic circulation (Batalin, 1958; Istoshin, 1960; Stepanov, 1961; Vasiliev and Makashin, 1991; Vanin, 2004), deep upwelling can be caused by processes such as the compensatory rise of water due to winter slope convection (Leonov, 1948; Stepanov, 1961; Yarichin and Pokudov, 1982), subsidence in the southern and southeastern regions of a sea due to compaction during mixing of cold and warm subtropical waters from the Sea of Japan in frontal sections, and the development of anticyclonic eddy formations (Yarichin and Pokudov, 1982; Yurasov and Yarichin, 1991). Using buoys drifting at a depth of 800 m, it was found that the nature of deep large-scale circulation in the Japan Basin is generally the same as in the surface layer, with the deep waters being covered by cyclonic motion throughout the year. In addition, it was revealed that within the LSCG, in its western and eastern parts, there are two areas of smaller-scale cyclonic activity—the western and eastern cyclonic gyres (WCG and ECG) (Danchenkov et al., 2005), with which upwellings of deep waters are inextricably linked. Drift of buoys in the western part of LSCG showed that the center of WCG was located at a point with coordinates 41°30′ N and 134°00′ E. The diameter of the cyclonic drift zone of buoys was usually about 30 miles, but "sometimes the cyclonic movement of a buoy occurred over a large area ..." (Danchenkov et al., 2005). Numerous calculations of currents (Leonov, 1960; Pokudov and Tunegolovets, 1975; Yurasov and Yarichin, 1991; Yoon et al., 2005; Trusenkova, 2007; Yurasov et al., 2011; Nikitin et al., 2012) have shown that the WCG can be located in different places in the band 40°00′–42°30′ N and 130°00′–136°00′ E, which is probably associated not only with the peculiarities of calculations, but also with the circulation variability. Nevertheless, due to the lack of research, it is still possible to judge the approximate location of WCG, with the central part of which the maximum influence of rising deep waters on the upper layer of the sea is associated. Another cyclonic region in the LSCG is the northern cyclonic gyre (NCG), which, according to the results of dynamic calculations, is clearly manifested off the coast of Primorye between 43°–46° N and 135°–139° E against the background of the coastal upwelling development and the inflow of Tsushima waters from Hokkaido Island (Nikitin et al., 2012, 2020). In the surface geostrophic circulation schemes constructed on the basis of data for the period from 1925 to 2005 (Nikitin et al., 2012), all three cyclonic circulations—the WCG, ECG, and NCG, differing in size and location of centers from season to season—are present in the large-scale cyclonic gyre (LSCG) region year-round.

In the 1990s, in the LSCG area, a winter intensification of the dynamics of deep waters with an increase in the velocity of deep current from minimum values in October to maximum values in March was also detected using stationary autonomous buoy stations and drifting deep buoys. Intensification covered the entire deep layer from 500 to 3000 m, in which measurements were taken (Takematsu et al., 1999a, 1999b; Senjyu et al., 2005; Choi and Yoon, 2010). This feature is much weaker in the cyclonic gyres of the southern half of a sea (Choi and Yoon, 2010). The winter intensification of the deep current may be caused by wind stress and thermohaline effects. However, as the authors argue (Yoon et al., 2005; Choi and Yoon, 2010; Trusenkova, 2018), these factors are not able to directly increase the velocity of deep currents. Nevertheless, wind and thermal effects can probably indirectly affect deep circulation (Trusenkova, 2018). The most established hypothesis about the strengthening of deep circulation in the winter period in the Japan Basin area is associated with the impact of synoptic eddies on the entire thickness of the sea. This hypothesis was a consequence of experimental observations and model calculations (Takematsu et al., 1999a, 1999b; Hogan and Hurlburt, 2000; Yoon et al., 2005; Choi and Yoon, 2010; Trusenkova, 2018). However, the mechanism for the increase in deep water velocity from October to March and its further decrease until October has not yet been established (Choi and Yoon, 2010).

Another phenomenon that may be associated with the intensification of deep circulation in the sea in the northern half in winter, according to the authors (Takematsu et al., 1999a; Trusenkova, 2007), is the slope convection and open sea convection developing during the winter (Talley et al., 2003; Lobanov et al., 2019). Within the framework of such a year-round phenomenon as deep upwelling, the intensification of deep circulation in the northern half of a sea in winter was not considered. Thus, in this paper, based on the analysis results of infrared (IR) satellite images and materials of ship hydrological surveys conducted by the authors of the article in different years, we consider the surface thermal structures of the northern part of the Sea of Japan detected by the satellite method, deep upwelling in the LSCG region, its relationship with synoptic-scale eddies, and the intensification of deep circulation in the northern half of the sea.

MATERIALS AND METHODS

Satellite Data

In this work, the thermal and eddy fields of the northern part of the Sea of Japan are analyzed using SST maps from the NOAA satellites obtained at the Center for Collective Use of the Regional Satellite Monitoring of the Environment of the Institute of Automation and Control Processes, Far Eastern Branch, Russian Academy of Sciences (IACP FEB RAS, Vladivostok) and posted online at http://www.satellite.dvo.ru. The methodology of main provisions for processing and analyzing satellite images are set out in the works (*Rekomendatsii*…, 1984; *Metodicheskie*…, 1987; Aleksanin and Aleksanina, 2006) and are based on visual decoding of IR images together with the analysis of ship data. Most attention was focused on the study of elements of satellite SST maps such as the genesis of thermal meso- and macrostructures, their position, size, shape, temperature levels, and its variability. The identification of eddies in satellite images was based primarily on their main features, such as roundness or arcuate shape with varying degrees of annularity manifestation or the spirality of their structure (*Rekomendatsii*…, 1984; Nikitin and Yurasov, 2008).

Hydrological Ship Data and Measurements at the Bottom Station

Figure 1 shows the schemes of hydrological surveys we carried out on October 2–21, 2019, on the R/V *Akademik Oparin* (cruise no. 57) and on December 7–28, 2021, on the R/V *Akademik Lavrentyev* (cruise no. 97). Most of sections were carried out to the border of the Russian Federation economic zone. CTD soundings on all sections were carried out with an SBE 9plus profiler to a depth of 1000–1500 m. On the section along 134° E in December 2021, measurements were carried out to the bottom with a maximum probing depth of 3550 m. The article also uses measurement data from the monitoring section along 134° E, which we also carried out to the bottom in December 2020 during the expedition of the R/V *Akademik Oparin* (cruise no. 62). The location of CTD sounding stations on the monitoring section along 134° E in 2020 practically coincides with the location of stations on this section during the survey in 2021, shown in Fig. 1b. Data of another deep-water section located in the NCG with the edge coordinates of 44°57′ N, 137°00′ E, and 44°05′ N, 138°20′ E and carried out on the R/V *Akademik Oparin* (cruise no. 58) on November 12–13, 2019, are also used in the work (Fig. 8). The location of the section is shown in Fig. 2 in the image of November 12, 2019, by a black segment. Visualization of the distributions of hydrological parameters in the work was performed using the Ocean Date View program (Schlitzer, 2019). This work also uses temperature and salinity data obtained using an SBE-37 meter installed in the bottom layer off the coast of southern Primorye at a monitoring bottom station at a depth of 22 m (marked with a triangle in Fig. 1a).

RESEARCH RESULTS

Emergence of Anomalous Thermal Regions

Satellite IR images shown in Fig. 2 show that, by October 2019, when the ship survey was carried out (October 2–21), two areas of low temperatures had already formed in the northern part of the sea, separated by the Tsushima water influx from Hokkaido Island. For the first time, anomalous areas with temperatures of 15°C and below clearly appeared in the SST field on September 18. In the SST images of October 9, 15, and 23, the anomalous areas have approximately the same shape and temperature, which dropped to 10–14°C. In the images of November 12 and 28, two areas with approximately the same shape and area as in October, but with temperatures already below 10°C and 5°C, respectively, are also preserved in the SST field. The appearance of anomalous thermal areas coincided with the development of coastal wind upwelling, which began, according to the temperature and salinity variability data at our bottom monitoring station located at a depth of 22 m off the coast of southern Primorye, on September 12 (Fig. 3). A steady decrease in bottom temperature lasted until October 7 (Fig. 3). As a result, the temperature decreased from 18.7 to 1.8°C, and the salinity increased from 32.38 PSU to 34.02 PSU (earlier in 2003–2007 (Sergeev et al., 2008), an approximate simultaneity of the onset of a decrease in bottom temperature during upwelling off the coast of southern and eastern Primorye was established; therefore, the results of one station allow us to assess the development of Primorsky upwelling along the coast to 44° N).

Then, from October 7 to 25, the upwelling relaxation process was observed. Temperature began to increase and reached a maximum value of 12.2°C, while the salinity decreased to 33.46 PSU. Then, the temperature decreased again and the salinity increased. By November 28, the temperature decreased to 1.8°C and continued to decrease further, while the salinity increased and exceeded 34.00 PSU. All this indicates the upwelling process continuation after the relaxation period. Practical invariance of shape, area, and temperature of the anomalous regions indicates that the coastal upwelling relaxation on October 7–25 did not significantly affect the SST field structure observed in October on satellite IR images. The surface temperature structure stability in October allows the surface temperature map, constructed using shipboard hydrological survey data carried out over a relatively long period from October 2–21 (Fig. 4a), to be considered as being in fairly good agreement with the satellite SST maps for October and, along with satellite IR images, to be used for the analysis of hydrological conditions.

Features of Deep Upwelling in the WCG Region

In October 2019, the hydrological situation to the south of Primorye, according to satellite IR images of SST and ship measurements, was characterized by lower temperatures relative to seaward areas and eddy formations surrounding the work area (Fig. 4a). Minimum temperatures (below 11°C) on the surface are observed near the coast, which is due to wind upwelling developing here in the autumn (Fig. 3). A frontal zone formed between the area with lower temperatures

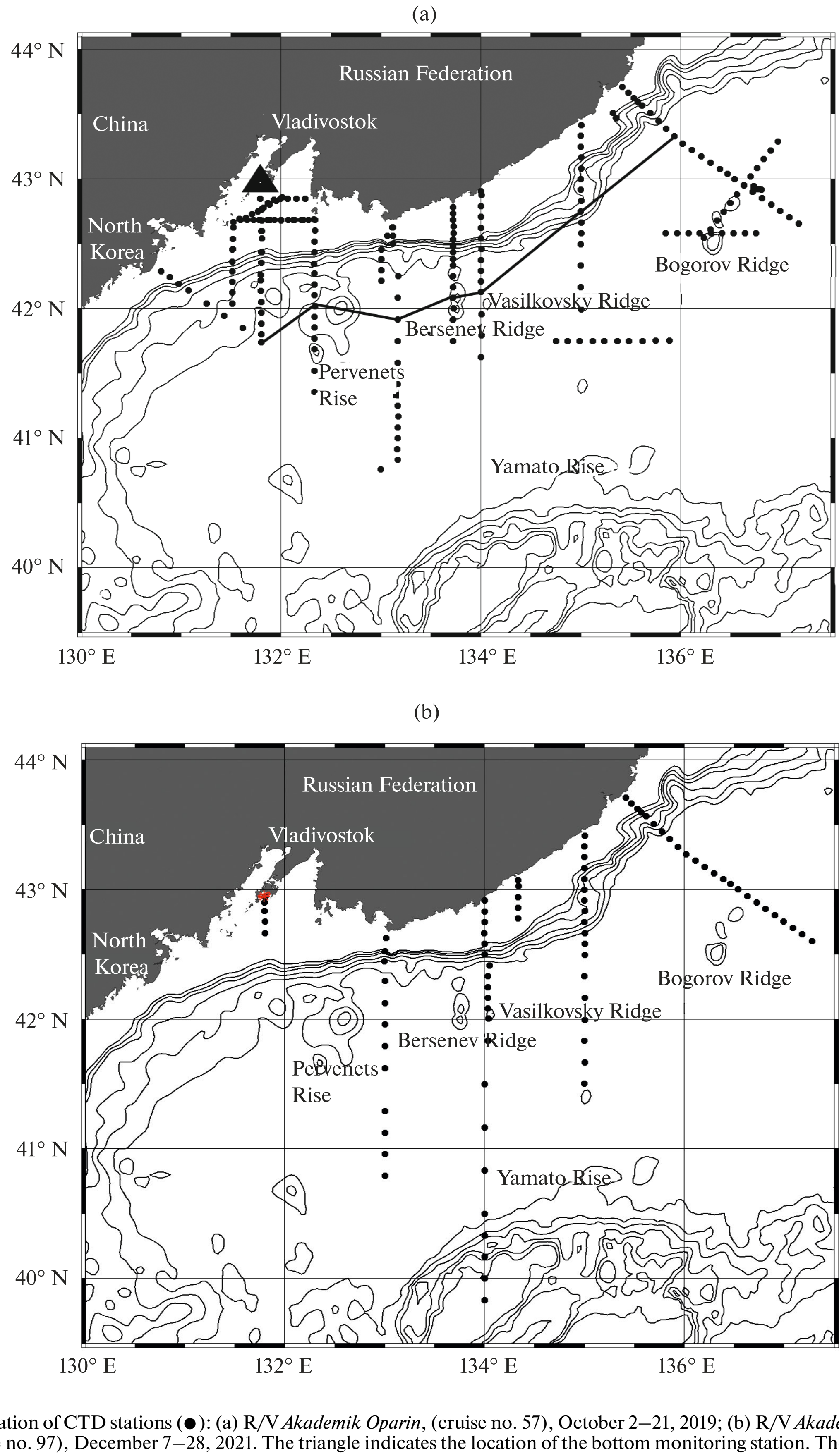

Fig. 1. Location of CTD stations (●): (a) R/V *Akademik Oparin*, (cruise no. 57), October 2–21, 2019; (b) R/V *Akademik Lavrentyev* (cruise no. 97), December 7–28, 2021. The triangle indicates the location of the bottom monitoring station. The broken line shows the northeastern section location.

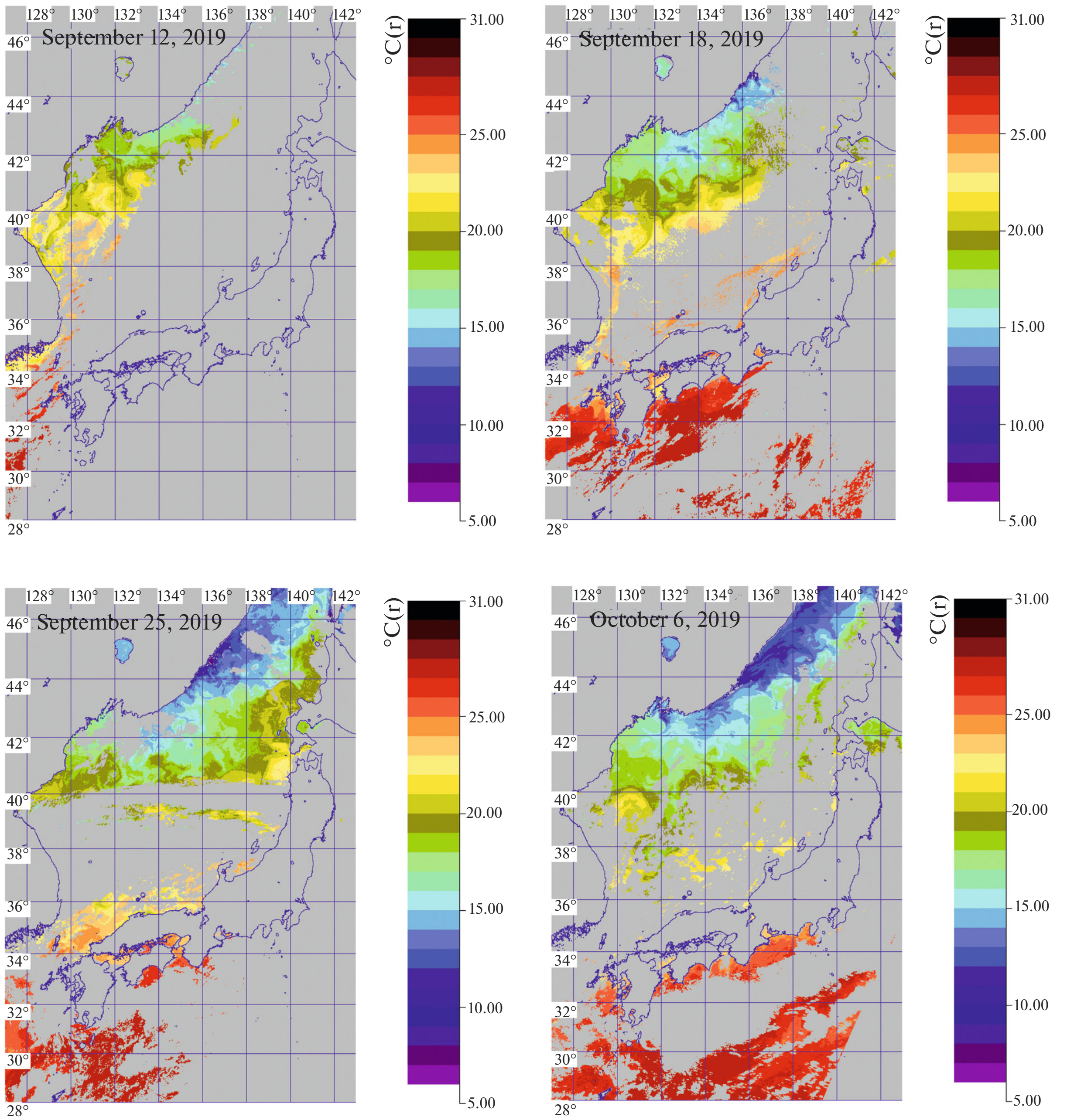

Fig. 2. Thermal structure of surface of the Sea of Japan based on satellite IR images in September to November 2019 and December 2021. In September and October, the temperature scales range from 5°C to 31°C and, in November and December, from 0 to 26°C. In the image from November 12, 2019, the black segment indicates the section, the results of which are shown in Fig. 8.

and eddies. The central part of the work area on the areal temperature distributions from the lower sounding horizon (1000 m) to the 100-m horizon is contoured by closed isotherms forming approximately identical elliptical dual-core areas with lower temperatures relative to neighboring areas (Figs. 4b, 4c).

On the meridional and quasi-zonal sections crossing the study area respectively along 134° E (Fig. 5a) and from the southwest from 41°45′ N and 131°48′ E to the northeast to 43°20′ N and 135°56′ E (Fig. 5b), a dome-shaped rise of isotherms with a common apex in the region of 42° N between the meridians of 132° E and 134.5° E is observed, which indicates an ascent of deep waters from the lower measurement horizons and almost to the surface (approximately to 50 m). As a result of the ascent of deep waters, areas with lower temperatures relative to neighboring areas were formed in the areal distributions (Figs. 4b, 4c). In the northeastern section (Fig. 5b), the two peaks are observed in the deep upwelling structure. To construct the northeastern section, shown by the broken line in

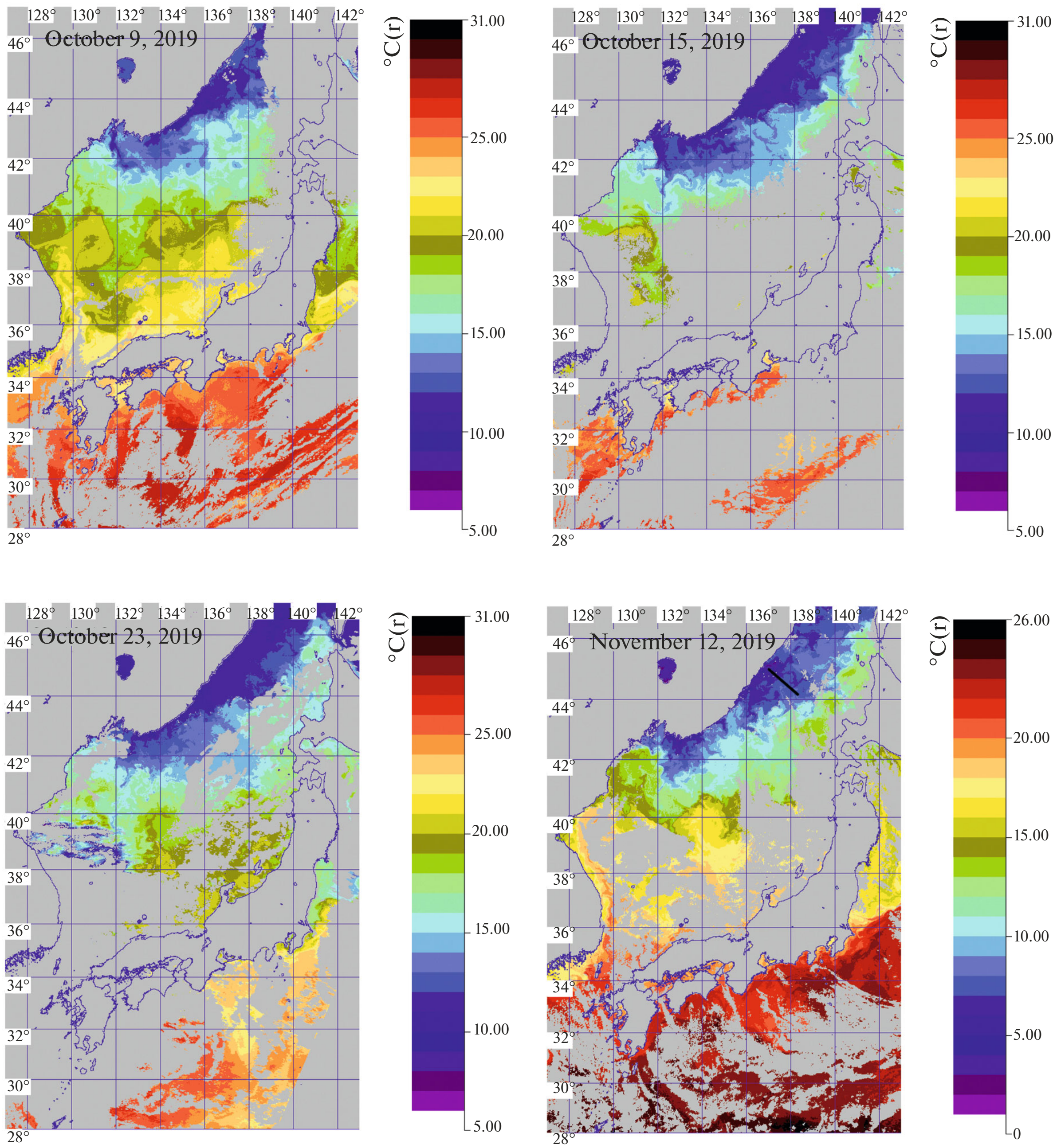

Fig. 2. (Contd.)

Fig. 1a, a station was selected on each of the seven sections used, at which the maximum rise in isotherms was observed on the section. Therefore, the northeastern section of the temperature distribution is a vertical section passing along a two-peak temperature ridge.

A notable feature of deep upwelling identified in the study area is that the axial line passing through the central region of deep water rise, identified by the minimum temperatures in the areal distributions (Figs. 4b, 4c), and directed from the southwest to the northeast, coincides with the line of the location of Pervenets underwater rise and the Bersenev and Vasilkovsky ridges (Fig. 4d). A similar feature was also revealed based on the data of December 2021 expedition on the R/V *Akademik Lavrentyev* (cruise no. 97) (Fig. 1b). Figures 6a and 6b show the areal temperature distributions at horizons of 300 and 1000 m, respectively. Unfortunately, due to unfavorable weather conditions, it was not possible to complete a section along 132° E and further west, which affected the quality of constructed temperature fields. Nevertheless, the temperature field shows that, in December 2021, in the deep layers above the Pervenets Rise and the Bersenev and Vasilkovsky ridges in the area of 42° N

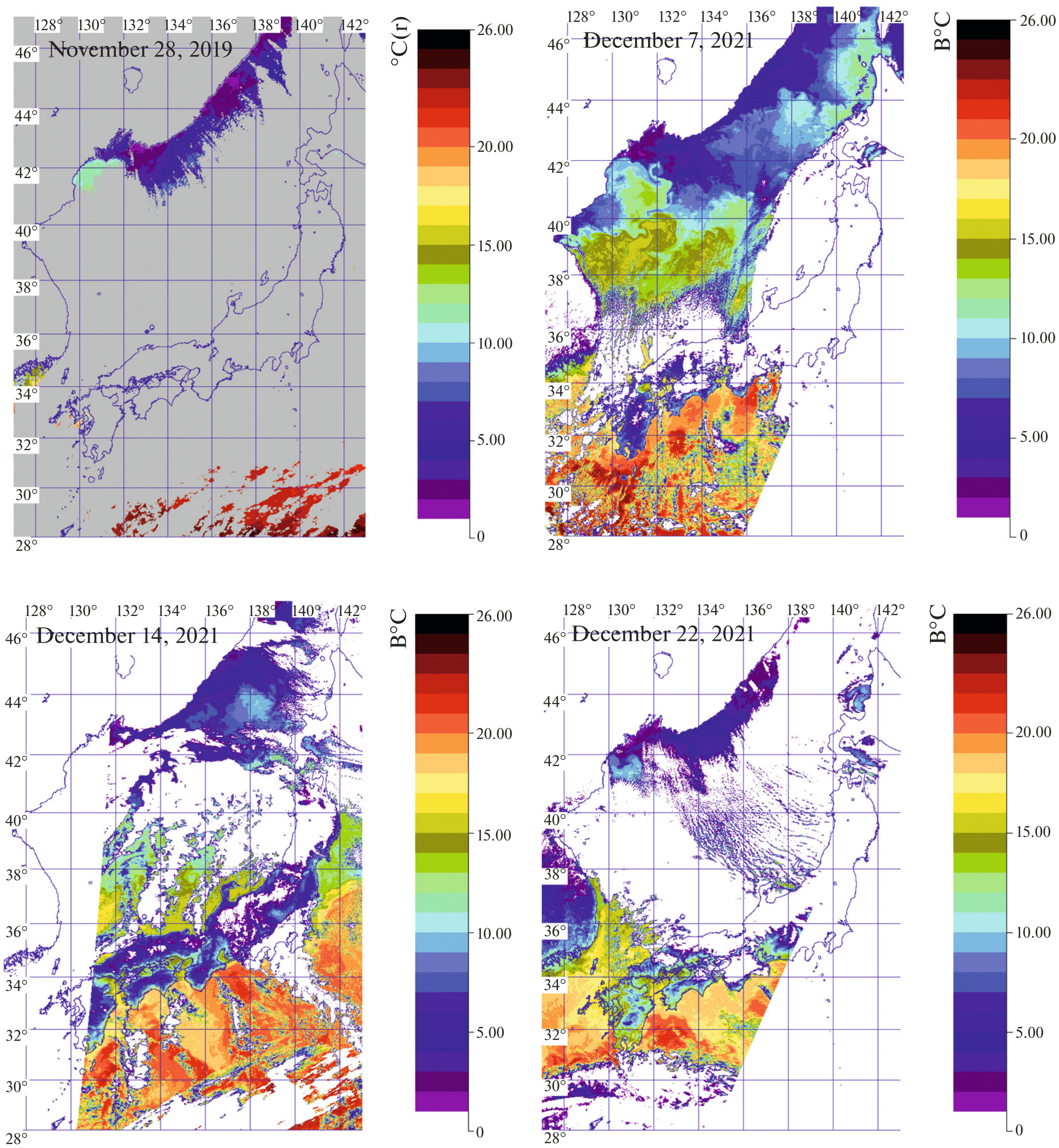

Fig. 2. (Contd.)

between 132° and 134.5° E, structures similar to those observed in October 2019 are distinguished (Figs. 4b, 4c; 6a, 6b). All this indicates the location of deep upwelling central region of the northwestern part of the sea here. The upwelling region extends further to the northeast to 135.5° E, deviating more and more towards the coast, as in October 2019, and forming another core of water upwelling in the area of 43° N and 135° E. The choice of 300 m horizon when constructing the areal temperature distribution in December 2021 (Fig. 6a) is due to the fact that, at this depth, the quasi-closure of isotherms is clearly manifested, in contrast to the overlying horizons, where the picture begins to fade due to the intensification of processes in the upper layer in December. Nevertheless, in December 2021, during our survey in the northwestern part of the sea, where deep upwelling is observed, the existence of a southwestern region of low temperatures is clearly visible on satellite IR images (Fig. 2).

Evidence that the rise of water starts from the bottom and spreads to the surface layer is the temperature distribution on the section along 134° E, which was, as noted above, carried out in the period from December 7 to 11, 2021, to the bottom (Fig. 7a). In the figure, above the Vasilkovsky Ridge, located on the line of the section with the top at approximately a depth of 1800 m (the depth at the base is 3200 m) at 42°05′ N, a pronounced rise in isotherms is observed. The same rise in isotherms from the bottom to the surface layer is observed above the Vasilkovsky Ridge on the section along 134° E, which we carried out a year earlier on the R/V *Akademik Oparin* (cruise no. 62) on December 20–26, 2020 (Fig. 7b). In general, the structure of the temperature field on the sections along 134° E is the same, differing mainly in a stronger deformation of the temperature field in December 2021 due to the deep anticyclone E (Figs. 7a, 7b) in the southern half of the section and two small near-slope eddy formations with centers at 42°20′ and 42°30′ N (Fig. 7a). Note also that, in Figs. 7a and 7b, the depth above the Vasilkovsky Ridge on the sections differs from the actual value due to the ship drift, which makes it difficult to carry out CTD stations exactly above the top.

Another remarkable feature of deep upwelling is that the central region of the deep water upwelling, extended from the southwest to the northeast, spreading further and further to the northeast to 135.5° E and deviating more and more towards the coast in the direction of Olga Bay, approximately coincides with the divergence zone noted earlier (Yarichin and Pokudov, 1982; Yarichin, 1982; Yurasov and Yarichin, 1991), which also deviates towards the coast in the direction of Olga Bay, like the upwelling zone. This divergence (Vasiliev and Makashin, 1991), according to the results of diagnostic calculation of the integral circulation, is associated with the upwelling of waters in the region of cyclonic vorticity. In Figs. 4b, 4c, 6a, and 6b, the structure of the temperature field in the form of closed isotherms in the region of 42° N indicates not only upwelling, but also the presence of a cyclonic gyre here. The presence of cyclonic circulation in the area of work on underwater bottom uplifts is confirmed by the distribution of zonal components of geostrophic velocity on sections along 134° E (Figs. 7c, 7d). One feature of the distribution of zonal components of geostrophic velocity on sections is its increased values in the area of the anticyclone in the southern half of the section in Fig. 7a, which clearly indicates the role of eddies in increasing the velocity of currents in the sea deep layer.

In Figs. 7c and 7d, it is clearly seen that zero isotaches separate the western and eastern flows in the area of the upwelling peak and the Vasilkovsky Ridge. Hence, the cyclonic gyre associated with the deep upwelling, located in the WCG area, is a large topographic eddy, probably formed during the interaction of incoming flow with positive forms of the bottom relief (Kozlov and Darnitsky, 1981; Zyryanov, 1995; Darnitsky, 2010)—the Vasilkovsky and Bersenev ridges and the Pervenets Rise. The greater part of the western coastal flow—the Primorsky Current—flows around the rises from the north, forming the northern

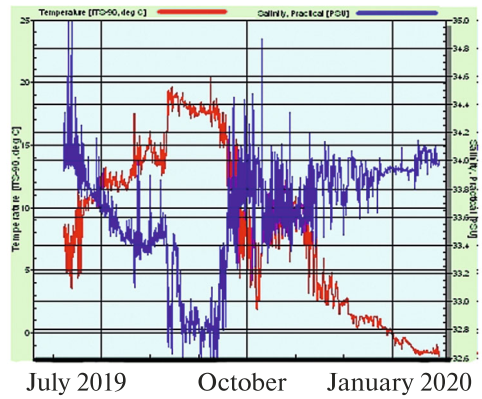

Fig. 3. Variability of temperature (red) and salinity (blue) at the bottom (22 m) monitoring station installed on June 7, 2019, in the coastal zone of southern Primorye southwest of Russky Island.

periphery of the LSCG and WCG—its western structure. In the topographic eddy structure, two small cyclonic eddies are distinguished, the centers of which are associated with two peaks of deep upwelling in Figs. 4b and 4c. These peaks are also distinguished in the temperature distribution in the northeastern section in Fig. 5b. One eddy is formed over the Vasilkovsky and Bersenev ridges; the second is located between the Pervenets Rise and the Bersenev Ridge (Figs. 4b, 4c, 6a, 6b). The experimental identification of the topographic factor in the cyclonic gyre formation and upwelling in the western part of the LSCG occurred in the autumn and winter seasons. At the moment, there are no similar studies in the spring–summer period, which does not allow us to draw unambiguous conclusions about the relationship between the factors of cyclonic vorticity and topography in the origin of deep upwelling and the seasonal variability of its location.

Deep Upwelling in the Northeastern Low Temperature Region

As was noted at the beginning of the article, in the northeastern region of low temperature off the coast of Primorye, identified on the basis of satellite images approximately between 43° and 46° N and 135° and 139° E, in the field of surface geostrophic circulation (Nikitin et al., 2012, 2020), another small cyclonic gyre—the northern (NCG)—is revealed in the area of the LSCG. In November 2019, on the R/V *Akademik Oparin* (cruise no. 58), a hydrological section to the bottom was made in this area (Fig. 8), the location of which is shown in Fig. 2 in the image of November 12, 2019, by a black segment. This section is perpendicular to the coastline and currents off the eastern coast of Primorye. The section shows a rise of water from the bottom to the surface, with deep upwelling shifted to the continental slope. The presence of a cyclonic gyre

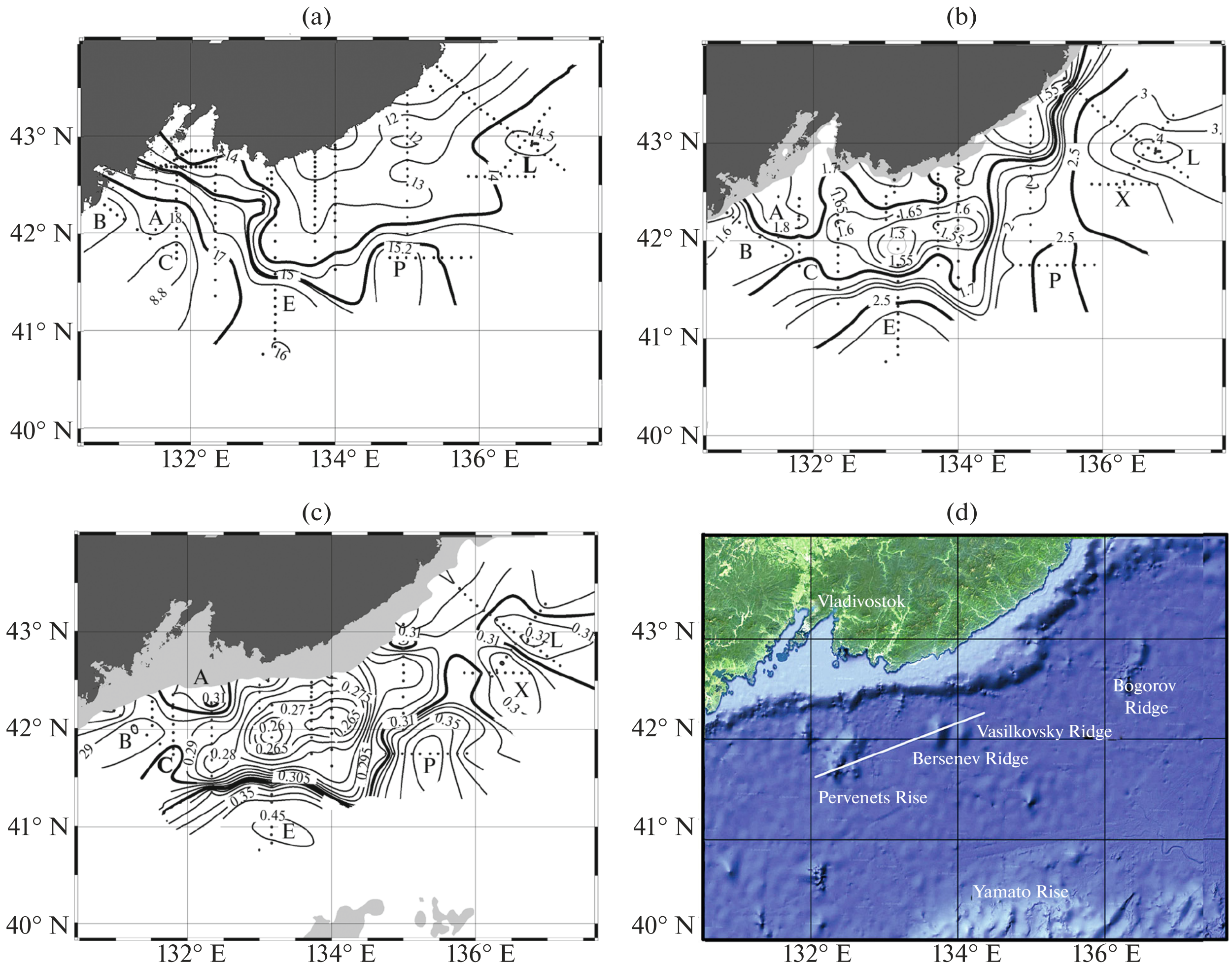

Fig. 4. Distribution of potential water temperature in October 2019 on the surface (a) and at 100 m (b) and 1000 m (c) horizons; bottom relief of the study area—white line passing through the Pervenets Rise and the Bersenev and Vasilkovsky ridges, coinciding with the axial line of the area of maximum rise of deep waters, identified by the minimum temperatures in (b) and (c–d). Points are the location of stations. Eddy formations are indicated by letters in (a, b, c).

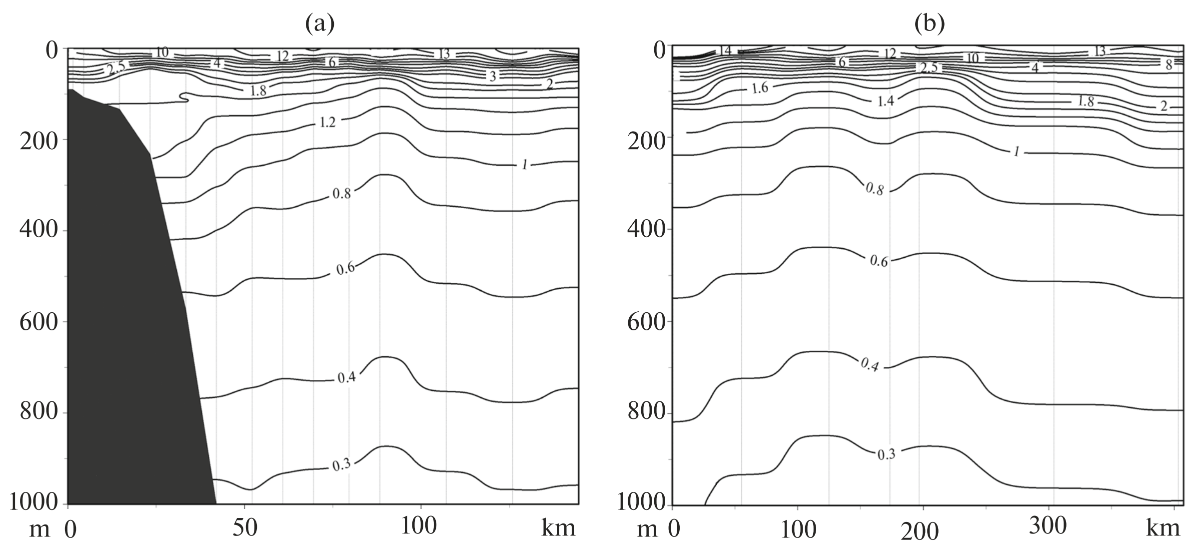

Fig. 5. Distribution of potential temperature along the 134° E section (a) and along the section directed from southwest to northeast (Fig. 1a) through the central region of deep upwelling (b) in October 2019. Vertical thin lines indicate the location of the stations.

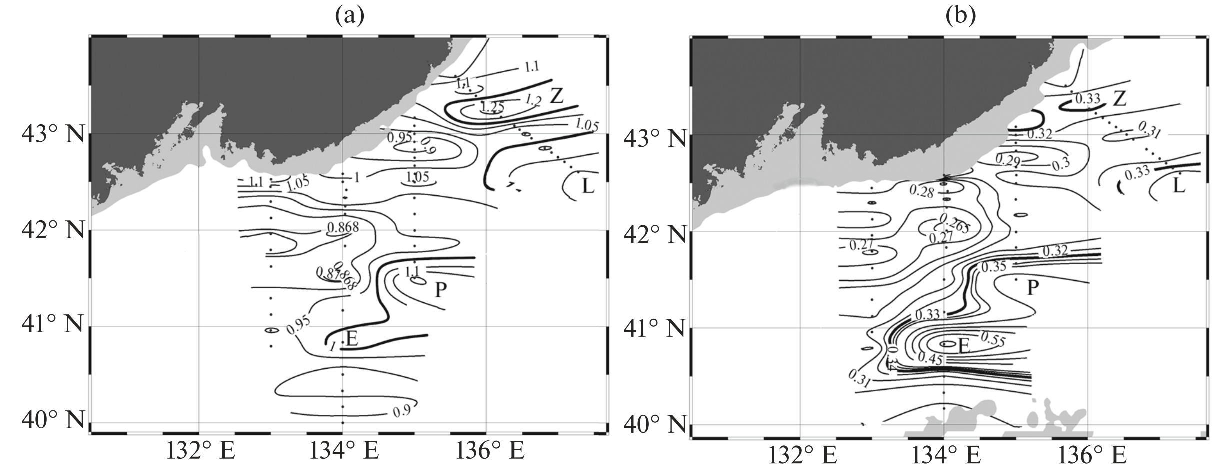

Fig. 6. Potential temperature distributions at 300 m (a) and 1000 m (b) horizons in December 2021. Points indicate station locations. Letters in (a) and (b) indicate eddy formations.

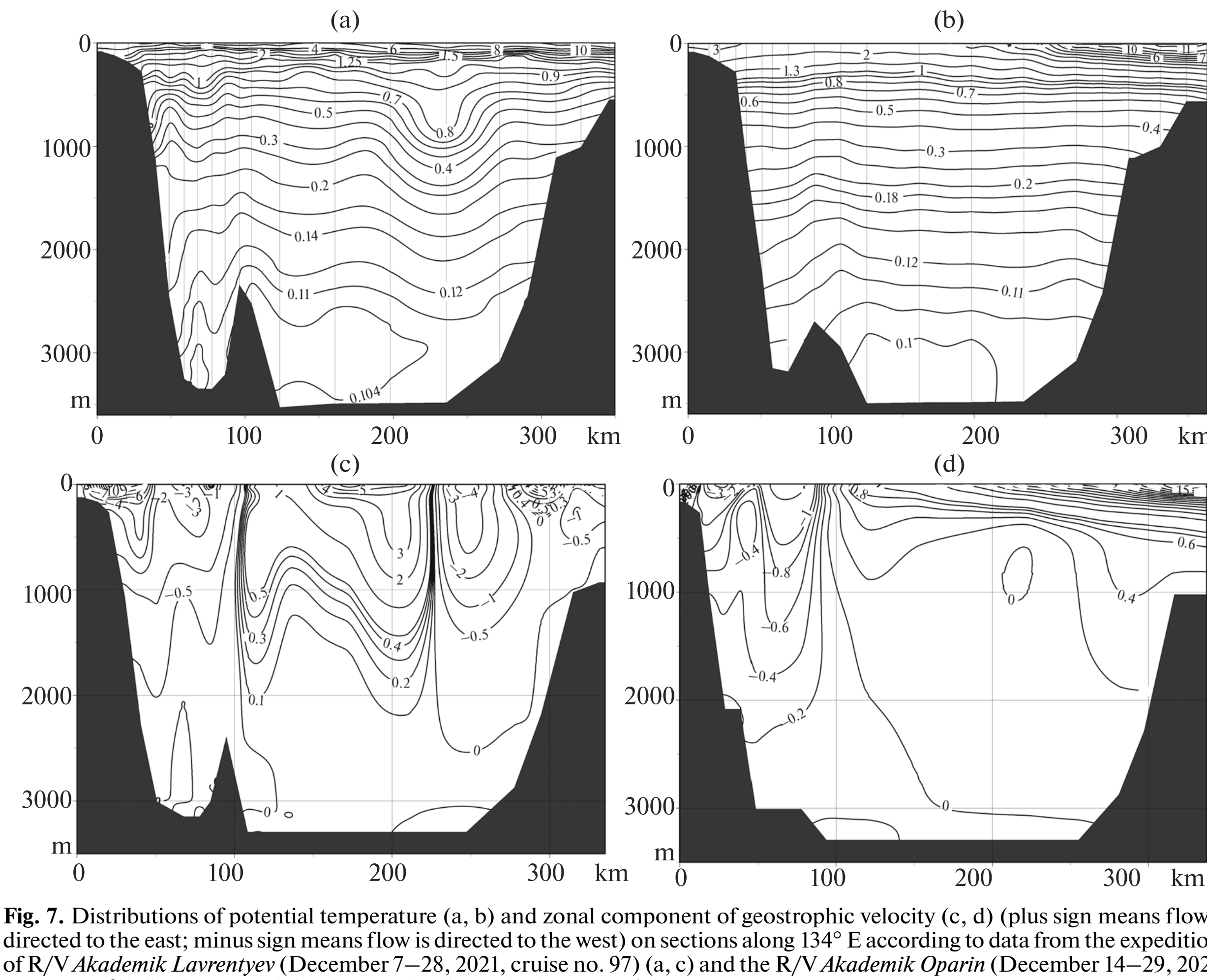

Fig. 7. Distributions of potential temperature (a, b) and zonal component of geostrophic velocity (c, d) (plus sign means flow is directed to the east; minus sign means flow is directed to the west) on sections along 134° E according to data from the expeditions of R/V *Akademik Lavrentyev* (December 7–28, 2021, cruise no. 97) (a, c) and the R/V *Akademik Oparin* (December 14–29, 2020, cruise no. 62) (b, d). Vertical thin lines in (a, b) are the location of the stations.

in the northeastern region of the low temperature off the coast of Primorye in November 2019 is confirmed by southwestern near the coast and northeastern offshore geostraphic flows (Fig. 8b), as well as the presence of a front formed by Tsushima warm waters and waters of the anomalous region and encircling the latter, which is clearly visible on the satellite SST maps for November 12 and 28, 2019 (Fig. 2).

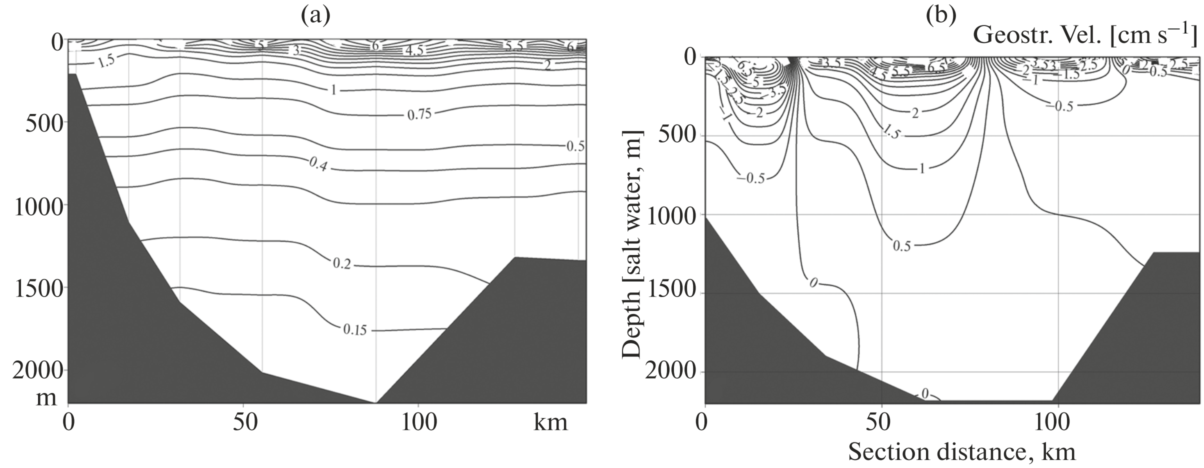

Fig. 8. Distribution of potential temperature (a) and velocity of geostraphic currents perpendicular to the section made on November 11–12, 2019, during the expedition of R/V *Akademik Oparin* (cruise no. 58) in the northeastern region of low temperature (b). The plus sign indicates the flow is directed to the northeast; the minus sign indicates the flow is directed to the southwest. Vertical thin lines in (a) are the location of the stations. Section is shown on the satellite image of November 12, 2019, in Fig. 2.

Role of Deep Upwelling and Eddies in the Intensification of Deep Circulation

In October 2019, the western cyclonic gyre (WCG) established in the area of underwater seafloor uplifts was surrounded by four eddy regions from the west, south, southeast, and east, in which five main anticyclonic eddies can be distinguished: A, C, E, P, and L, observed from the surface to the lower measurement horizon (1000 m) (Figs. 4a, 4b, 4c). These eddies are clearly visible in the satellite IR image of October 9, 2019 (Fig. 9a). In December 2021, the central upwelling area was also surrounded by anticyclonic eddies located in approximately the same places: eddy E is located to the south of the central part of the upwelling, P is to the southeast, and L is to the east. The coastal eddy Z is located to the northwest of eddy L (Figs. 6a, 6b). For eddies, we use the same designations as in the eddy arrangement diagram constructed by the authors (Nikitin and Yurasov, 2008) based on satellite data for 1988–1996 (Fig. 9b). In our work and in the article (Nikitin and Yurasov, 2008), the positions of eddies of the same name (A, C, E, P, and L) generally coincide, which indicates the existence of a certain pattern in the arrangement of eddies in the form of a quasi-latitudinal eddy belt surrounding the WCG region from the seaward side. Let us call it a small eddy belt, or SEB. This anticyclonic belt has a small "defect" in the form of a cyclonic topographic eddy X located between anticyclones P and L over the Bogorov Ridge (Figs. 4b, 4c, 4d) (Lobanov et al., 2021). Anticyclonic formations A, C, E, P, and L in the northern half of the sea are closely associated with quasi-meridional eddy chains, which, in turn, are fairly stable structural formations observed throughout the year and located in approximately the same places. Chains and the warm subtropical waters associated with them are oriented approximately along 131°, 134°, and 137° E, and in the eastern part of the sea, between 42°–44° N from 139° E to 135° E (Nikitin et al., 2002; Nikitin and Yurasov, 2008; Prantz et al., 2018). In our case, in October 2019, the chains retained the structure and direction as noted above. The chain at 131° E, consisting of eddies G, D, C, B, and A, was oriented to the north, and the directions of chains at 134° E, including eddies Y2 and E, and at 137° E with eddies N, M, and P, were slightly deviated to the northwest, but generally agreed with the above-mentioned features of the location of eddy chains and the routes of propagation of subtropical waters to the northern part of the sea (Fig. 9a). The chain located in the northeastern part of the LSCG consists of eddies L and, presumably, S and T (Fig. 9a). The region of formation of these eddies (Fig. 9b) is located in the northern part of the sea to the north of 43° N between 138°–140° E (Nikitin and Yurasov, 2008). This shift in the chain in the southwest direction in October 2019 is probably associated with the occurrence of wind-driven coastal upwelling and the development of northern cyclonic gyre (NCG) adjacent to the coast of Primorye between 43° and 46° N (Fig. 9a).

The most important element of the Sea of Japan chains are seven large quasi-stationary anticyclonic formations (Nikitin and Yurasov, 2008), of which five (B, G, Y2, N, and L) surround the western and eastern gyres in the LSCG region (Fig. 9). Moreover, the eddies B, G, Y2, and N, surrounding the LSCG from the west and south, form their own quasi-latitudinal vortex belt—the large eddy belt (LEB). In the satellite image from October 9, 2019, during the period of our work, the quasi-stationary eddies B, G, Y2, N, and L can be distinguished (Fig. 9a), the location of which approximately coincides with the location of eddies in the diagram (Fig. 9b) of the authors (Nikitin et al.,

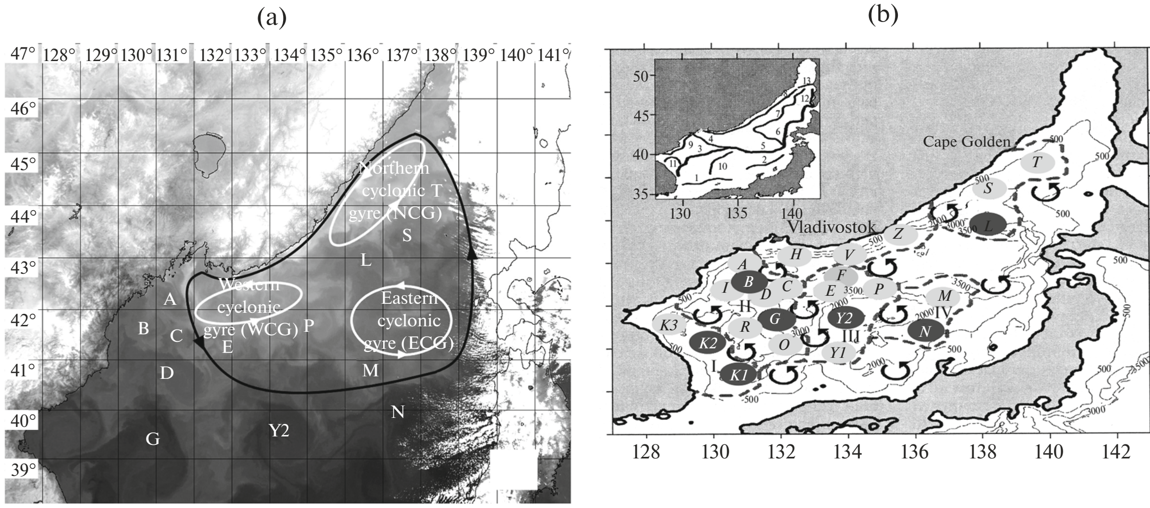

Fig. 9. (a) Image of the northern half of the Sea of Japan in the IR range from the NOAA satellite for October 9, 2019. Letters in the figure indicate anticyclonic eddy formations; black line outlines the LSCG region; and white lines indicate cyclonic gyres: western (WCG), eastern (ECG), and northern (NCG). (b) Figure from (Nikitin and Yurasov, 2008). Letters in the figure indicate anticyclones established based on satellite data for 1988–1996. Dark circles indicate quasi-stationary anticyclones. The inset is a generalized diagram of surface thermal fronts in the Sea of Japan.

2002; Nikitin and Yurasov, 2008), with the exception of eddy L, which shifted from the formation area at approximately coordinates 44° N and 138° E (Nikitin et al., 2012) to a point with coordinates 43° N and 137° E. Quasistationary eddies are the source of jet emissions or an intermediate link for the entrainment of jets with further transfer of the invading subtropical waters to other eddies of the chain located to the north, which have a smaller diameter and lifespan, but extend vertically almost to the bottom (Lobanov et al., 2007; Nikitin and Yurasov, 2008). The subarctic front passes along the northern periphery of quasi-stationary eddies, forming the LEB (Nikitin et al., 2012). Moreover, the frontal subarctic zone is formed from the waters of the LSCG from the north and from the subtropical waters of the LEB from the south. Similarly, the SEB interacts with the WCG, forming its own front (Figs. 4a, 4b, 4c). The interaction is carried out by unidirectional flows of the southern periphery of the WCG and the northern periphery of the SEB eddies. Along the northern periphery of L, S, and T eddies, which form another small eddy belt, there is a front separating the waters of the NCG and the waters of the said eddies. In the work (Nikitin et al., 2012), the maximum geostraphic velocities were observed on this front in November 2003. The same picture was observed according to calculations for May 2013 (Nikitin et al., 2020). Eastern cyclonic gyre (ECG), identified in 1990s using buoys (Danchenkov et al., 2005), is surrounded on three sides by eddies (N, M, P, L, and S) in the image of October 9, 2019, the peripheries of which also form a local front zone with unidirectional flows with gyre waters. Thus, eddy belts and cyclonic gyres are inextricably linked and interact with unidirectional flows.

In December–February, in the subarctic zone of the sea, an intensification of LSCG is observed in the upper layer (Takematsu et al., 1999a; Kang et al., 2000; Trusenkova et al., 2007; Taranova et al., 2018) and, accordingly, the gyres included in it, which is due to positive wind tangent stress curl values and the strengthening of northerly winds from autumn to winter. Strengthening of cyclonic gyres leads to the intensification of upwellings associated with gyres in the upper layer. At the same time, the close interaction of gyres and vortex belts should also affect the dynamics of eddies included in the belts. In the framework of hypothesis on the eddy nature of the deep circulation intensification (Hogan and Hurlburt, 2000) in the northern half of a sea in winter, the possible intensification of eddies is only part of mechanism for increasing the velocity of deep waters from October to March. The intensification of gyres in winter, leading to increased upwelling in the upper layer, also intensifies the vertical and transverse horizontal circulation, in particular, in the WCG. Figure 10 shows a simplified scheme of vertical circulation on the section along 134° E in December 2021, constructed on the temperature distribution basis in Fig. 7a. The structure of the vertical circulation on the section crossing the WCG and the SEB anticyclonic eddy from the south, as well as a small anticyclonic eddy between the coast and the WCG from the north, is a set of circulation cells. Cells cover the entire water column with multidirectional vertical and transverse horizontal circulation, which forms in the WCG upper layer and anticyclonic eddies, respectively, zones of divergence and convergence of waters, and in the lower layer, respectively, zones of convergence and divergence. It is evident from Fig. 10 that the upwelling intensification in

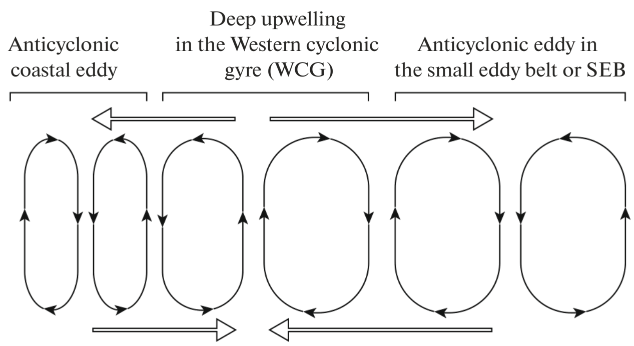

Fig. 10. Simplified diagram of vertical circulation along the 134° E section in December 2021.

the upper layer will intensify the convergence of waters in the lower layer, increasing the flow velocity. This intensification on the seaward side of the WCG is carried out through the anticyclonic eddy, which, spreading to the bottom, deforms the bottom convective layer and the upwelling region in the temperature field (Fig. 7a). The greatest contribution to the intensification of deep circulation in the region of the Japan Basin in the winter period is probably associated with the compensatory eddy flow of energy and water mass from the upper layers to the deep ones under conditions of deep upwelling intensifying from autumn to winter. The intensification nature, a monotonous increase in the average velocity of deep waters from a minimum in October to a maximum in March (Choi and Yoon, 2010), is probably determined by the peculiarity of the development of vertical and transverse horizontal circulation, which occurs gradually as vortex energy and the compensatory flow of overlying waters into the deep layers are pumped up throughout the winter period under conditions of the ongoing strengthening of northwest winds by February–March until the change from winter to summer monsoon.

CONCLUSIONS

Satellite IR images, hydrological surveys, and measurements at a monitoring bottom station in the coastal zone of southern Primorye made it possible to identify and examine poorly studied features of the structure and dynamics of waters in the northern half of the Sea of Japan in the autumn–winter periods of 2019–2021. One of these features is the annual formation of two anomalous thermal areas in large-scale cyclonic gyre (LSCG) in the autumn–winter period. This phenomenon is observed after the summer monsoon change to the winter one and the occurrence of autumn wind coastal upwelling. The location of these thermal structures coincides with the location of western (WCG) and northern (NCG) cyclonic gyres, which are inextricably linked with deep upwelling. Deep upwelling in the northwestern Sea of Japan extends from the bottom to the surface layer, focusing along the axial line passing through the Pervenets Rise and the Bersenev and Vasilkovsky ridges in the region of 42° N between 132° and 135.5° E. The upwelling area, extending towards the coast towards Olga Bay, approximately coincides with the divergence zone in the western part of large-scale cyclonic gyre (LSCG)—the water area where the small western cyclonic gyre (SWCG) is located. The WCG, associated with deep-water upwelling, is a large topographic eddy, probably formed by the interaction of the Primorsky Current with positive bottom relief forms—the Vasilkovsky and Bersenev ridges and the Pervenets Rise.

A deep-water section in the northeastern low-temperature region, where the NCG is also observed, showed that deep-water upwelling in this part of the LSCG is displaced onto the continental slope.

In the autumn–winter period, the LSCG and its small cyclonic gyres, the WCG, the ECG, and the NCG, are surrounded by large and small eddy belts (LEBs and SEBs) formed by quasi-meridional vortex chains. Gyres and belts are inextricably linked and form frontal zones on the periphery, in which they interact by unidirectional flows. It is assumed, within the framework of the hypothesis on the vortex nature of the intensification of deep circulation (Hogan and Hurlburt, 2000), that the interaction of vortex belts with cyclonic gyres leads to an increase in deep circulation in the winter period. The peculiarity of the variability of the velocity of deep waters—an increase from October to March, is probably due to the nature of the development of vertical and transverse horizontal circulation in the system of cyclonic gyres—eddy belts as a result of the intensification of deep upwelling with the strengthening of northern winds in the winter period.

FUNDING

This work was carried out as part of the State Budget R&D theme of the Il'ichev Pacific Oceanological Institute, Far Eastern Branch, Russian Academy of Sciences, for 2023 on the topic "Study of the Main Processes Determining the State and Variability of the Oceanological Characteristics of the Marginal Seas of Asia and Adjacent Areas of the Pacific and Indian Oceans," reg. number 121021700346-7.

CONFLICT OF INTEREST

The authors of this work declare that they have no conflicts of interest.

REFERENCES

Aleksanin, A.I. and Aleksanina, M.G., Monitoring of the thermal structures of the ocean surface using the data of infrared channels of NOAA satellites on the example of the Kuril region of the Pacific Ocean, *Sovrem. Probl. Distantsionnogo Zondirovaniya Zemli Kosmosa*, 2006, vol. 3, no. 2, pp. 9–15.

Batalin, A.M., Density, in *Gidrologicheskii spravochnik morei SSSR* (Hydrological Handbook of the USSR Seas), Leningrad: Gidrometeoizdat, 1958, vol. 8, no. 2, pp. 244–263.

Choi, Y.J. and Yoon, J.-H., Structure and seasonal variability of the deep mean circulation of the East Sea (Sea of Japan), *J. Oceanogr.*, 2010, vol. 66, no. 3, pp. 349–361.

Danchenkov, M.A., Riser, S.C., and Yoon, J.-H., Deep currents of the central Sea of Japan, *Podvodnye Tekhnol. Mir Okeana*, 2005, no. 3, pp. 58–63.

Darnitskii, V.B., *Okeanologicheskie protsessy vblizi podvodnykh gor i khrebtov otkrytogo okeana* (Oceanological Processes Near Seamounts and Open Ocean Ridges), Vladivostok: TINRO-Tsentr, 2010.

Goncharenko, I.A., Federyakov, V.G., Lazaryuk, A.Yu., and Ponomarev, V.I., Thematic processing of AVHRR data for coastal upwelling, *Issled. Zemli Kosmosa*, 1993, no. 2, pp. 97–108.

Hogan, P.J. and Hurlburt, H.E., Impact of upper ocean–topographical coupling and isopycnal out-cropping in Japan/East Sea models with 1/8° to 1/64° resolution, *J. Phys. Oceanogr.*, 2000, vol. 30, no. 10, pp. 2535–2561.

Istoshin, Yu.V., Water temperature of Sea of Japan and the possibility of its forecast, *Tr. Okeanogr. Kom. Akad. Nauk SSSR*, 1960, vol. 7, pp. 52–97.

Kang, S.K., Seung, Y.H., Park, J.J., Park, J.-H., Lee, J.H., Kim, E.J., Kim, Y.H., and Suk, M.-S., Seasonal variability in middepth gyral circulation patterns in the central East/Japan Sea as revealed by long-term Argo data, *J. Phys. Oceanogr.*, 2000, vol. 46, pp. 937–946. https://doi.org/10.1175/JPO-D-15-0157.1

Kozlov, V.F. and Darnitskii, V.B., Topographic cyclogenesis in the ocean, *Tr. Dal'nevost. Nauchno-Issled. Gidrometeorol. Inst.*, 1981, no. 83, pp. 85–100.

Leonov, A.K., Water masses of the Sea of Japan, *Meteorol. Gidrol.*, 1948, no. 6, pp. 61–78.

Leonov, A.K., The Sea of Japan, in *Regional'naya Okeanografiya* (Regional Oceanography), Leningrad: Gidrometeoizdat, 1960, vol. 1, pp. 291–463.

Lobanov, V.B., Ponomarev, V.I., Salyuk, A.N., Tishchenko, P.Ya., and Tully, L.D., The structure and dynamics of synoptic eddies in the northern part of the Sea of Japan, in *Dal'nevostochnye morya Rossii* (Far Eastern Seas of Russia), vol. 1: *Okeanologicheskie issledovaniya* (Oceanological Research), Akulichev, V.A., Ed., Moscow: Nauka, 2007, pp. 450–473.

Lobanov, V.B., Sergeev, A.F., Navrotskii, V.V., Voronin, A.A., Gorin, I.I., and Pavlova, E.P., Instrumental observations of cascading on the slope of Peter the Great Bay, Sea of Japan, in *Trudy konferentsii: "Sovremennye metody i sredstva okeanologicheskikh issledovanii" (MSOI- 2019)* (Proceedings of the Conference "Modern Methods and Tools of Oceanological Research" (MTOR-2019)), Moscow: IO RAN, 2019, vol. 1, pp. 104–108.

Lobanov, V.B., Sergeev, A.F., Shlyk, N.V., Voronin, A.A., Gorin, I.I., Tsoi, V., Goryachev, V.A., Krainikov, G.A., Zverev, S.A., Rudykh, Ya.N., Mar'ina, E.N., Prushkovskaya, I.A., Luk'yanova, N.B., and Telichko, A.S., Synoptic water dynamics in the northwestern part of the Sea of Japan in the fall period (according to the results of the 57th cruise of the Akademik Oparin research vessel, in *Fizika geosfer. Dvennadtsatyi Vserossiiskii simpozium* (Physics of the Geospheres. Twelfth All-Russian Symposium), Vladivostok, 2021, pp. 71–73. https://www.poi.dvo.ru/conf/phg2021.

Metodicheskie ukazaniya po kompleksnomu ispol'zovaniyu sputnikovoi informatsii dlya izucheniya morei (Methodical Instructions for the Integrated Use of Satellite Data for Marine Research), Leningrad: Gidrometeoizdat. 1987.

Mokievskaya, V.V., Chemical characteristics of water masses, in *Osnovnye cherty geologii i gidrologii Yaponskogo morya* (Main Features of Geology and Hydrology of the Sea of Japan), Stepanov, V.N., Moscow: Izd. AN SSSR, 1961, pp. 122–131.

Nikitin, A.A. and Yurasov, G.I., Synoptic eddies of the Sea of Japan according to satellite data, *Issled. Zemli Kosmosa*, 2008, no. 5, pp. 42–57.

Nikitin, A.A. and Yurasov, G.I., Surface thermal fronts in the Sea of Japan, *Izv. Tikhookean. Nauchno-Issled. Inst. Rybn. Khoz. Okeanogr.*, 2017, vol. 148, pp. 170–192.

Nikitin, A.A., Lobanov, V.B., and Danchenkov, M.A., Possible paths of the tropical water transport to the region of the Far Eastern marine natural park, *Izv. Tikhookean. Nauchno-Issled. Inst. Rybn. Khoz. Okeanogr.*, 2002, vol. 131, pp. 41–53.

Nikitin, A.A., Danchenkov, M.A., Lobanov, V.B., and Yurasov, G.I., A new mechanism for the surface circulation of the Sea of Japan taking into account synoptic eddies, *Izv. Tikhookean. Nauchno-Issled. Inst. Rybn. Khoz. Okeanogr.*, 2009, vol. 157, pp. 158–167.

Nikitin, A.A., Yurasov, G.I., and Vanin, N.S., Satellite observations of synoptic eddies and the geostrophic circulation of the Sea of Japan waters, *Izv., Atmos. Ocean. Phys.*, 2012, no. 48, no. 9, pp. 980–992.

Nikitin, A.A., Djakov, B.S., and Kapshiter, A.V., The Primorskoe Current at standard sections and in satellite images of the Sea of Japan's surface, *Izv., Atmos. Ocean. Phys.*, 2020, no. 56, no. 12, pp. 1605–1614.

Panfilova, S.G., Water temperature, in in *Osnovnye cherty geologii i gidrologii Yaponskogo morya* (Main Features of Geology and Hydrology of the Sea of Japan), Stepanov, V.N., Moscow: Izd. AN SSSR, 1961, pp. 155–169.

Pokudov, V.V. and Tunegolovets, V.P., New mechanism of currents in the Sea of Japan for the winter period, *Tr. Dal'nevost. Nauchno-Issled. Gidrometeorol. Inst.*, 1975, no. 60, pp. 74–115.

Pokudov, V.V., Man'ko, A.N., and Khlusov, A.N., Features of the hydrological regime of the waters of the Sea of Japan in winter, *Tr. Dal'nevost. Nauchno-Issled. Gidrometeorol. Inst.*, 1976, no. 60, pp. 74–115.

Prants, S.V., Uleysky, M.Yu., and Budyansky, M.V., Lagrangian analysis of transport pathways of subtropical water to the Primorye coast, *Dokl. Earth. Sci.*, 2018, vol. 481, no. 2, pp. 1099–1103.

Rekomendatsii po ispol'zovaniyu sputnikovykh IK snimkov v okeanologicheskikh issledovaniyakh (Recommendations for the Use of Satellite IR Images in Oceanological Studies), Vladivostok. TINRO. 1984.

Schlitzer, R., Ocean Date View, 2019. https://odv.awi.de.

Senjyu, T., Shin, H.-R., Yoon, J.-H., Nagano, Z., An, H.-S., Byun, S.-K., and Lee, C.-K., Deep flow field in the Japan/East Sea as deduced from direct current measurements, *Deep Sea Res. II*, 2005, vol. 52, nos. 11–13, pp. 1726–1741.

Sergeev, A.F., Matveev, V.I., Lobanov, V.B., Gorin, I.I., Kotenko, B.M., and Starikov, A.G., Variability of the near-bottom water temperature in the coastal zone of Primorye in 2003–2007, in *Tezisy dokladov Tret'ei Mezhdunarodnoi nauchno-prakticheskoi konferentsii "Morskie pribrezhnye ekosistemy. Vodorosli, bespozvonochnye i produkty ikh pererabotki*" (Abstracts of the Third International Scientific and Practical Conference "Sea Coast Ecosystems. Algae, Invertebrates, and Their Processing Products"), Vladivostok. TINRO-Tsentr, 2008, pp. 207–208.

Stepanov, V.N., General characteristics of the hydrology of the Sea of Japan, in *Osnovnye cherty geologii i gidrologii Yaponskogo morya* (Main Features of Geology and Hydrology of the Sea of Japan), Stepanov, V.N., Moscow: Izd. AN SSSR, 1961, pp. 102–107.

Takematsu, M., Nagano, Z., Ostrovskii, A.G., Kim, K., and Volkov, Y., Direct measurements of deep currents in the northern Japan Sea, *J. Oceanogr.*, 1999a, vol. 55, no. 2, pp. 207–216.

Takematsu, M., Ostrovskii, A.G., and Nagano, Z., Observations of eddies in the Japan basin interior, *J. Oceanogr.*, 1999b, vol. 55, no. 2, pp. 237–246.

Talley, L.D., Tishchenko, P., Luchin, V., Nedashkovskiy, A., Sagalaev, S., Kang, D.-J., Warner, M., and Min, D.-H., Atlas of Japan (East) Sea hydrographic properties in summer, 1999: Supplementary material, *Progr. Oceanogr.*, 2004, vol. 61, nos. 2–4, pp. 277–348. https://doi.org/10.1016/j.pocean.2004.06.011

Talley, L.D., Lobanov, V., Ponomarev, V., Salyuk, A., Tishchenko, P., Zhabin, I., and Riser, S., Deep convection and brine rejection in the Japan Sea, *Geophys. Res. Lett.*, 2003, vol. 30, no. 4, pp. 1–4. https://doi.org/10.1029/2002GL016451

Taranova, S.N., Yurasov, G.I., and Zhabin, I.A., Seasonal variability of surface water circulation in the northern part of the Sea of Japan according to drifting buoy data, *Izv. Tikhookean. Nauchno-Issled. Inst. Rybn. Khoz. Okeanogr.*, 2018, vol. 192, pp. 177–183.

Trusenkova, O.O., Modeling of deep currents in the Sea of Japan: Relationship with currents in the pycnocline, *Izv. Tikhookean. Nauchno-Issled. Inst. Rybn. Khoz. Okeanogr.*, 2018, vol. 192, pp. 184–201.

Trusenkova, O.O., Seasonal and interannual changes in water circulation in the Sea of Japan, in *Dal'nevostochnye morya Rossii* (Far Eastern Seas of Russia), vol. 1: *Okeanologicheskie issledovaniya* (Oceanological Research), Akulichev, V.A., Ed., Moscow: Nauka, 2007, pp. 280–306.

Trusenkova, O.O., Stanichnyi, S.V., and Ratner, Yu.B., Major variability modes and wind patterns over the Sea of Japan and adjacent areas, *Izv., Atmos. Ocean. Phys.*, 2007, vol. 43, no. 5, pp. 634–648.

Vanin, N.S., Anomalous thermal conditions in the northwestern part of the Sea of Japan in fall 2003, *Izv. TINRO*, 2004, vol. 138, pp. 345–354.

Vasil'ev, A.S. and Makashin, V.P., Ventilation of waters of the Sea of Japan in winter, *Meteorol. Gidrol.*, 1991, no. 2, pp. 71–79.

Yarichin, V.G., Some features of horizontal water movement in the Sea of Japan north of 40° N, *Tr. Dal'nevost. Nauchno-Issled. Gidrometeorol. Inst.*, 1982, no. 96, pp. 111–121.

Yarichin, V.G. and Pokudov, V.V., Formation of structural features of the hydrophysical fields and currents in the northern deepwater part of the Sea of Japan, *Tr. Dal'nevost. Nauchno-Issled. Gidrometeorol. Inst.*, 1982, no. 96, pp. 86–95.

Yoon, J.-H., Abe, K., Ogata, T., and Wakamatsu, Y., The effects of wind-stress curl on the Japan/East Sea circulation, *Deep Sea Res. II*, 2005, vol. 52, nos. 11–13, pp. 1827–1844.

Yurasov G.I. Features of the structure and dynamics of waters in the northern part of the Sea of Japan, Vladivostok: Far East Oceanological Institut, Far East Scientific Center, USSR Acad. Sci., 1995, VINITI Dep. no. 468-B95, January 27, 1995.

Yurasov, G.I. and Yarichin, V.G., *Techeniya Yaponskogo morya* (Currents of the Sea of Japan), Vladivostok: Izd. DVO AN SSSR, 1991.

Yurasov, G.I., Vanin, N.S., and Rudykh, N.I., Climatic characteristics of currents in the Sea of Japan according to calculations using the dynamic method, *Izv. Tikhookean. Nauchno-Issled. Inst. Rybn. Khoz. Okeanogr.*, 2011, vol. 164, pp. 340–347.

Zhabin, I.A., Gramm-Osipova, O.L., and Yurasov, G.I., Wind upwelling off the northwestern coast of the Sea of Japan, *Meteorol. Gidrol.*, 1993, no. 10, pp. 82–86.

Zyryanov, V.N., *Topograficheskie vikhri v dinamike morskikh techenii* (Topographic Eddies in the Dynamics of Sea Currents), Moscow: IVP RAS, 1995.

Translated by V. Selikhanovich